RSC Advances

ROYAL SOCIETY OF CHEMISTRY

www.rsc.org/advances

Microwave-assisted synthesis of Au/CdS nanorods for visible-light responsive photocatalyst

Jihong Park[a], Sungmook Park[a], Rengaraj Selvaraj[b*] and Younghun Kim[a*]

[a]Department of Chemical Engineering, Kwangwoon University, Wolgye-dong, Nowon-gu, Seoul 139-701, Republic of Korea

[b]Department of Chemistry, Sultan Qaboos University, P.C. 123, Al0Khoudh, Muscat, Sultanate of Oman

*

* Co-corresponding author. E-mail address: srengaraj@squ.edu.om (R. Selvaraj)

* Corresponding author. Tel.: +82-2-940-5769; fax: +82-2-941-5769.

E-mail address: korea1@kw.ac.kr (Y. Kim)

Abstract

In this work, cadmium sulfide (CdS) is suggested as visible-light responsive photocatalysts with narrow band gap (2.42 eV). CdS nanorods were synthesized by a facile and rapid microwave-assisted method and Au dots were decorated on the surface by a reduction method. The additions of the Au dots hinder the recombination of electron-hole pair and enhance the photocatalytic activity under visible light. The photocatalytic activity of Au/CdS nanorods was evaluated by the photodegradation of methylene blue (MB) under visible light irradiation (455 nm LED lamp). The photocatalytic efficiency of Au/CdS nanorods is compared to conventional TiO_2 (P25) and CdS-A prepared by autoclave method, and an improvement of the Au/CdS system attributed to the reduced band gap energy (2.31 eV) and enhanced absorption in the range of 400 to 800 nm was observed. The calculated mineralization ratio of MB by Au/CdS nanorods showed higher compared to data presented in literature. This facile and efficient synthesis route may promote the utilization of Au/CdS nanorods as visible light photocatalysts.

1. Introduction

Considerable attention is being paid to semiconductor photocatalysis for decomposition of pollutants during water treatment. Conventionally, TiO_2 is used to eliminate organic pollutants in wastewater treatment plant due to low cost, stability, and abundance.[1] As well-known limitation of TiO_2 is the wide band gap (3.2 eV) that limits operating conditions, i.e., working under UV irradiation.[2] Visible-light responsive photocatalysts, such as cadmium sulfide (CdS) systems, with narrow band gap have been suggested in literature.[3-5]

CdS, as an important II-VI semiconductor with a direct narrow band gap (2.42 eV) and large exciton binding energy, has very broad applications in light-emitting diodes, solar cells, and photocatalysts.[5-7] The morphology and size have significant influence on the physical and optical properties.[5] Nanostructured CdS such as spherical-shaped,[6] core-shell,[8] nanorods,[9] and hierarchical nanoscrystals[5] have been successfully prepared by hydrothermal process, thermal evaporation, microwave-assisted method, and template-based method.[5,10] Microwave hydrothermal approach is ideal to synthesize complicated CdS structures under mild conditions with shorter times and lower temperatures than common hydrothermal methods using autoclave.[1,5,7]

In this work, we synthesized Au-decorated CdS (Au/CdS)nanorods by microwave methods and evaluated photocatalytic activity via degradation of methylene blue (MB). In the autoclave method, the phase transformation of CdS is correlated to the preparation conditions, such as high pressure, high temperature or tedious time. Microwave-assisted synthesis of CdS simultaneously adjusts the phase and morphology at low temperature and

atmosphere pressure.[11]This synthetic approach does not require surfactant, template, or sophisticated equipments. Only ethlyenediamine, a widely used solvent, was utilized during the synthesis of CdS nanocrystals and control of the various morphologies.[10]To enhance the photocatalytic activities or adjust the optical properties of CdS nanocrystals, noble metals (Au, Ag, and Pt) can be decorated on the CdS.[9] In this work, Au was decorated as a spherical dot on the CdS nanorod by reduction method of the metal ion.[12]

The crystal structure, morphology and optical properties of Au/CdS and CdS nanorods were analyzed with X-ray diffraction (XRD), normal and high resolution transmission electron microscopy (TEM and HR-TEM), and ultraviolet diffuse reflectance spectroscopy (UV-DRS). Furthermore, the photocatalytic activities in the degradation of MB over the Au/CdS and CdS photocatalysts were also investigated under the visible-light irradiation (λ =450 nm, royal blue). To compare its activity, conventional TiO_2 photocatalyst (P25) and CdS nanorod prepared by autoclave method were also used to remediate the organic dye under visible-lighting.

2. Experimental section

2.1 Microwave-assisted synthesis of CdS nanorod

All source materials purchased from Sigma-Aldrich were of analytical grade and utilized as-received without further purification. CdS nanorod with high aspect ratio (*ca*. 10) was synthesized by microwave-assisted method. In a typical synthesis process, 0.266 g of 1 mM cadmium acetate hydrate ($Cd(CH_3COO)\cdot 2H_2O$) and 0.215 g of 3 mM thioaccetamide (CH_3CSNH_2) were dissolved in 50 mL of ethylenediamine ($NH_2C_2H_4NH_2$) to form a homogeneous solution at room temperature. After 30 min of stirring, the resulting solution was transferred into a 100 mL Teflon vessel, followed by microwave-heating and maintained 140°C for 1 hr in microwave reaction system (MARS6, CEM) with 1800 W and 2455 MHz of magnetron frequency. After the microwave process, Teflon vessel was cooled down naturally. The deep-yellow powders were collected by centrifugation with 10000 rpm for 5 min, and washed by deionized (DI) water and anhydrous ethanol three times, respectively. Finally, as-made CdS powders were dried at 60°C in drying oven for 8 h.

2.2 Decoration of Au dot on CdS nanorod

Gold (Au) nanocrystals were decorated directly onto the CdS nanorods by reduction of gold precursor ($HAuCl_4\cdot 3H_2O$) with sodium borohydride ($NaBH_4$). 1 mL of 2.5 mM Au precursorwas dissolved in 9 mL of ethylenediamine, and the resulting solution and 10 mg of CdS powder were mixed with 20 mL of 1 mM $NaBH_4$ dissolved in DI water. After 30 min of stirring, centrifugation, washing, and drying processes were conducted as described

previously in the synthesis of CdS nanorod. Finally, 1 wt% of Au dot decorated on the CdS nanorodswere obtained.

2.3 Photocatalytic degradation of organic dye (MB)

The photocatalytic activity of Au/CdS and CdS nanorods was evaluated by the photodegradation of methylene blue ($C_{16}H_{18}N_3SCl$) uder visible light irradiation at room temperature. A low powered visible LED lamp (36 W, UHP-Microscope-LED-450, Prizmatix) was used as the light source to provide visible light (λ =450 nm).As compared to arc-Xe lamp, LED lamp less increased of temperature of system during light irradiation. The photocatalytic tests were performed with 10 mg of Au/CdS and CdS nanorod suspended in MB aqueous solutions (100 mL, 5 mg/L). The suspension was stirred in the dark for 30 min to insure the adsorption/desorption equilibrium. At the given time intervals, about 1 mL of the suspension was taken for the following analysis after centrifugation. The concentration of MB left in the centrifuged aqueous solution was determined by UV-vis spectroscopy (UV-1800, Shimadzu). For comparison, the photocatalytic activities of commercial TiO_2 (Degussa P25, Evonik) and CdS-A nanorod prepared by autoclave method[13] were also tested at the same experimental conditions.

2.4 Characterizations

The crystalline structure and morphology of as-made Au/CdS and CdS nanorods were examined by XRD (SC222, PANalytical), TEM (JEM 1010, Jeol), and HR-TEM (JEM-3010, Jeol). Band gap energy was calculated by spectrum data analyzed with UV-DRS (V-670, JASCO).

3. Results and discussion

Semiconductor CdS photocatalysts are conventionally prepared by hydrothermal methods at high temperature and pressure for long processing times (> 24 hr). While microwave-assisted methods are simple and rapid synthetic processes for preparation of CdS nanostructures at room temperature, the crystallinity of as-made CdS nanoparticles significantly influences photocatalytic activities.[11]Therefore, the crystal structure was analyzed with XRD and Fig. 1 shows typical XRD patterns of CdS and CdS-A nanorods prepared by microwave-assisted methods and conventional autoclave methods, respectively. The strong and sharp diffraction peaks reveal high quality crystallization despite mild synthetic conditions. The crystallinity of CdS nanorods showed similar or sharper peaks compared to CdS-A nanorods prepared by hydrothermal methods using autoclave. All the diffraction peaks for CdS and CdS-A can be indexed to the standard hexagonal (wurtzite) phase of CdS with lattice parameters of a = 4.1 Å and c = 6.7 Å (JCPDS 41-1049).[11,13] No peaks from impurities and incorporation of the cubic phase are detected. The intensity ratios of the peaks corresponding to the (103) and (110) planes of the wurtzite structure are used to infer the phase composition of CdS nanocrystals.[10] While the (103)/(110) value of wurtzite CdS is in the range of 0.97 to 0.35, the planes ratio of CdS and CdS-A is about 0.51 and 0.28, respectively, indicating the crystal structure of CdS nanorods has higher crystallinity than CdS-A.

As observed by Saunders et al., the reflection corresponding to the (002) planes, which run perpendicular to the long axis of CdS and CdS-A nanorods, is narrower than the

(100) and (101) diffraction peaks due to the anisotropic nanoparticles shape.[9] In addition, the intensity of the (002) peak is higher than expected for spherical CdS nanoparticles.[11,14,15] This may be due to high crystallinity, large crystalline size, and anisotropic shape of CdS nanorods, indicating a preferential growth along the c-axis.[16] Although microwave-assisted preparation of CdS nanostructure effectively reduces the processing time, incomplete microwave treatment (under 1 h) leads to decreased crystallinity of as-made CdS.[7,17]

The morphology and microstructure of CdS were investigated using TEM and HR-TEM (Fig. 2). All CdS samples displayed a nanorod shape and TEM measurements indicated a thickness of CdS and CdS-A of ca. 20 nm and 10 nm, respectively. All CdS samples have high aspect ratio above 11, and the length of CdS (244.3 ±41.8 nm) was longer than CdS-A (147.3 ±15.3 nm), indicating the c-axis growth of CdS synthesized by microwave is more efficient. The hydrothermal temperature plays an important role in the formation of CdS,[10] efficient direct transfer of energy is more crucial in rapid synthesis of CdS nanorods. As mentioned by Hu et al., in microwave-assisted synthesis of CdS nanocrystals, rather than temperature, the irradiation time and concentration of ethylenediamine is key factor in determining the morphology of particle.[18] When CdS was prepared in DW phase using microwave, CdS showed aggregated morphology. Whereas, CdS prepared with 30 mL of ethylenediamine showed slightly rod-shape but aggregated morphology.

By XRD analysis, the average crystalline size of CdS and CdS-A nanorods was calculated to be ca.26.2 nm and 13.5 nm, respectively, on the basis of Scherrer's equation for the (002) reflection. The crystalline size calculated by XRD similar to the thickness of CdS nanorods, indicating the (002) plane determines the c-axis growth of CdS nanorods.

As growth in the c-axis direction of the CdS nanorod, strain induced in powders due to crystal imperfection and distortion may exist. The lattice strain was calculated using the Williamson and Hall (W-H) equation:[8,19] $B\cos\theta = 0.9\lambda/D + 4\eta\sin\theta$, where B is the full width at half-maximum, λ is wavelength of Cu$K\alpha$radiation, D is the crystallite size, and η is the effective strain. Based on the XRD data in Fig. 1, the effective strain was obtained from the slope of a plot of $B\cos\theta$ against$4\sin\theta$.The strain of CdS and CdS-A was a negative value,-0.09 and -0.24%, respectively, indicating compressive strain[8] and more relaxed in the larger crystallite size CdS as compared to CdS-A. Therefore, microwave treatment reduces the compressive strain during the growth of CdS nanorods in the c-axis direction. The crystallite size (thickness) for CdS and CdS-A by W-H equation is found to be 31.8 nm and 14.9 nm, respectively, which correlates with values obtained by XRD and TEM analysis.

As shown in Fig. 2b, Au dots were decorated on the (001) side of CdS nanorods. The size of Au dots was measured to be 9.8 ±1.3 nm, similar diameter as colloidal Au nanoparticles prepared in solution. Au dots loaded onto each CdS nanorod ranged from 5 to 8. Au dots pre-synthesized by reduction between reductant and Au precursor readily attached to the sides of as-synthesized CdS nanorods. Generally, growth of Au nanocrystal onto the end of CdS nanorod would require an interface between the $(022)_{Au}$ facet and the $(002)_{CdS}$ facet.[9] However, the rectangular lattice of the $(022)_{Au}$ facet would necessitate significant lattice distortion for epitaxial growth onto the hexagonal atomic arrangement of the $(002)_{CdS}$ facet. Therefore, Au growth or decoration onto the sides of CdS nanorod was preferred (Fig. 2b), providing a physical indication of the presence of defect sites.

HRTEM images (Fig. 2d) showed lattice fringes being perpendicular to the direction of nanorod growth. The lattice spacing (d) was measured as 0.332 nm, agreeing well with the

distance (0.334 nm) between the (002) planes of hexagonal CdS (JCPDS 41-1049). CdS nanorods appear to grow along the c-axis [001] direction, confirmed by XRD analysis.

The optical property of as-made CdS samples was investigated with UV-DRS as shown in Fig. 3. All CdS samples exhibit significant increase in the photoabsorption at wavelengths around 520 nm due to the intrinsic band gap transition (Fig. 3a). Compared to spherical CdS,[5] the absorption spectra of CdS nanorods show an enhanced absorption in the visible light region ranging from 400 nm to 800 nm. The optical absorption near band gap energy (E_g) was calculated using Tauc's formula: $(\alpha h\nu)^2=A(h\nu-E_g)$,[11] where $\alpha$is the absorption coefficient, $h\nu$ is incident photon energy, and A is a constant. Fig. 3b shows the plot of $(\alpha h\nu)^2$ versus ($h\nu$) for CdS, Au/CdS, and CdS-A nanorods. The band gaps of CdS have been calculated from the onset of the absorption edge, which are 2.36, 2.31, and 2.39 eV for CdS, Au/CdS, and CdS-A, respectively. Compared to the band gap of bulk CdS (2.42 eV at room temperature), a red shift of Au/CdS nanorods, attributed to the morphology of CdS nanocrystals,[5] occurs at 0.11 eV, as compared to CdS (0.06 eV) and CdS-A (0.03 eV). Such red shift of the absorption edge may be attributed to the internal stress induced by structural defects.[20]

The photocatalytic degradation of MB under visible light irradiation (450 nm LED) was conducted to evaluate the photocatalytic performance of CdS, Au/CdS, CdS-A, and P25 (Fig. 4). As exposure time is extended, the intensity of the characteristic peak at 664 nm of MB decreases dramatically and the absorption peaks become blue-shifted (Fig. 4a). When 3 mg/L of MB is exposed in the solution with 10 mg of Au/CdS, the degradation efficiency of MB reaches to 100% within 1 h. By calculating the mineralization ratio ($r = VC/m$), namely, effective degradation of MB (mg) by Au/CdS (mg) comparisons can be drawn to literature

data, where, *V*, *C*, and *m* is volume (100 mL) and concentration (3 mg/L) of MB, and mass (10 mg) of Au/CdS photocatalyst used, respectively. As-made Au/CdS nanorods showed a 0.03 ratio, and appeared higher compared to literature data: 0.0004 for reduced grapheme oxide (RGO)-CdS nanocomposite (rhodamine B, RhB),[16] 0.006 for CdS-TiO_2-RGO (methyl orange),[1] 0.0003 for TiO_2 (MB),[21] 0.01 for CdS cubic microsphere (MB and RhB),[11] and 0.003 for C/CdS hybrid sphere (RhB).[18] Therefore, Au/CdS nanorod prepared by microwave methodology may be a highly effective photocatalyst working under visible light.

The curves of the photodegradation of MB in the presence of different photocatalysts were plotted (Fig. 4b). Before irradiation of visible light, the suspension was stirred in the dark for 30 min to insure adsorption/desorption equilibrium. While MB adsorbed insignificantly on the CdS, Au/CdS, and P25 materials, 5% of initial concentration of MB adsorbed on the CdS-A sample. The order of photodegradation activity of MB in the four samples follows the following trend: Au/CdS > CdS-A > CdS > P25. For photodegradation of 5 mg/L of MB in 1 h, the degradation rate is approximately 75%, 65%, 60%, and 0% of initial MB, respectively. At 450 nm in the UV-DRS spectrum (Fig. 3a), the absorbance intensity of Au/CdS (1.063) is higher than CdS (0.975) and CdS-A (0.995). Au decorated on the CdS nanorod effectively enhanced the absorbance of bare CdS nanorods due to the absorption contribution of Au dots or effective inhibition of electron-hole recombination by modification of the fundamental process of electron-hole pair separation during irradiation.[1,16] When photocatalytic degradation of MB was conducted at 450 nm irradiation by LED lamp, photocatalytic activity of Au/CdS nanorods is higher than other samples.

In order to efficiently compare the photocatalytic activities of CdS samples, the apparent rate constant (k, min^{-1}) is calculated by pseudo-first-order kinetics: $ln(C/C_0)=kt$.[11] The values of k are 0.9×10^{-6} min^{-1}, 1.4×10^{-2} min^{-1}, 2.2×10^{-2} min^{-1}, and 1.6×10^{-2} min^{-1} for P25, CdS, Au/CdS, and CdS-A, respectively (inset box in Fig. 4b). Au/CdS nanorod has a higher rate constant as compared to reported data, 1.9×10^{-2} for CdS cubic microsphere (MB).[11]

Based on the photocatalytic results, the Au/CdS nanorod represented the highest photocatalytic activity among the three comparable systems, which may be attributed to the lower band gap energy and the weaker recombination rate of electron-hole under visible light. As illustrated in Fig. 5, both radicals and the holes are active oxidative species in the photodegradation of MB with Au/CdS nanorod, which is similar to the tentative mechanism of photodegradation of RhB with RGO-CdS.[16] Under visible light irradiation, charge separation in Au/CdS nanorod is initiated and Au dots on the CdS nanorod act as an electron acceptor to efficiently hinder the recombination of electron-hole pairs.[22] The superoxide anion radical and hydroxyl radical activates from dissolved oxygen and adsorbed water, respectively. Finally, the active species with strong oxidizes the MB molecule to CO_2, H_2O, or other small molecules.[11,16,21]

The stability of photocatalysts is important in practical application. In order to evaluate the stability of Au/CdS nanorods, a five-cycle photodegradation sequence for MB at the same initial concentrations was carried out, with each cycle lasting 60 min as shown in Fig. 6. No obvious deactivation of Au/CdS was found and the photodegradation efficiency after the 2^{nd} to 5^{th} run compared to the 1^{st} run was maintained around 95-100%. The Au/CdS nanorod prepared by microwave method a potentially attractive candidate as a

photocatalyst for water purification, has good repeatability and stability during photocatalysis.

4. Conclusions

In summary, a facile and rapid microwave-assisted method was applied to prepare CdS nanorods having hexagonal (wurtzite) phase. Though the synthetic conditions for microwave method are mild, the crystallinity of CdS nanorods is higher than CdS-A nanorods prepared by hydrothermal method using autoclave. The photocatalytic degradation of MB in aqueous under visible light irradiation showed that Au/CdS nanorod display superior photocatalytic performance to the other samples (CdS, CdS-A, and P25). The calculated mineralization ratio of MB by Au/CdS nanorods showed a value of 0.03, the highest value compared to literature data. The repeatability and stability of the photocatalytic behavior of Au/CdS makes for an attractive candidate photocatalyst for water purification under visible light condition.

Acknowledgement

This work was supported by the National Research Foundation of Korea (NRF-2010-0007050) and the Korea Environmental Industry & Technology Institute (201400140002).

References

1. T. Lv, L. Oang, X. Liu, T. Lu, G. Zhu, Z. Sun and C. Q. Sun, *Catal. Sci. Technol.*, 2012, **2**, 754.
2. S. Ebraheem and A. El-Saied, *Mater. Sci. Appl.*, 2013, **4**, 324.
3. R. Selvaraj, K. Qi, S. M. Z. Al-Kindy, M. Sillanpää, Y. Kim and C. W. Tai, *RSC Adv.*, 2014, **4**, 15371.
4. R.C. Pawar, V. Khare and C.S. Lee, *Dalton Transact*. 2014, **43**, 12514.
5. B. Hu, Z. Jing, J. Huang and J. Yun, *Trans. Nonferrous Met. Soc. China*, 2012, **22**, s89.
6. L. Zhu, T. Pan and Z. Xu, *ACS Appl. Mater. Interfaces*, 2011, **3**, 3146.
7. T. Xuan, J. Q. Liu, R. J. Xie, H. L. Li and Z. Sun, *Chem. Mater.*, 2015, **27**, 1187.
8. S. Khanchandani, S. Kundu, A. Patra and A. K. Ganguli, *J. Phys. Chem. C*, 2012, **116**, 23653.
9. E. Saunders, I. Popov and U. Banin, *J. Phys. Chem. B.*, 2006, **110**, 25421.
10. X. Wang, Z. Feng, D. Fan, F. Fan and C. Li, *Cryst. Growth Des.*, 2010, **10**, 5312.
11. C. Deng and X. Tian, *Mater. Res. Bull.*, 2013, **48**, 4344.
12. J. Roh, J. Yi and Y. Kim, *Langmuir*, 2010, **26**, 11621.
13. J. S. Roy, T. P. Majumder and R. Dabrowski, *J. Lumines.*, 2014, **148**, 330.
14. S. Karan and B. Malik, *J. Phys. Chem. C*, 2007, **111**, 16734.
15. S. Arora and S. S. Manoharan, *J. Phys. Chem. Solids*, 2007, **68**, 1897.
16. S. Kundu, H. Lee and H. Liang, *Inorg. Chem.*, 2009, **48**, 121.
17. J. J. Zhu, H. Wang, J. M. Zhu and J. Wang, *Mater. Sci. Eng. B*, 2002, **94**, 136.
18. Y. Hu, Y. Liu, H. Qian, Z. Li and J. Chen, *Langmuir*, 2010, **26**, 18570.

19. V. D. Mote, Y. Purushotham and B. N. Dole, *J. Theoret. Appl. Phys.*, 2012, **6**, 6.

20. Z. Y. Wang, X. S. Fang, Q. F. Lu, C. H. Ye and L. D. Zhang, *Appl. Phys. Lett.*, 2006, **88**, 083102.

21. A. Houas, H. Lachheb, M. Ksibi, E. Elaloui, C. Guillard and J. M. Herrmann, *Appl. Catal. B: Environ.*, 2001, **31**, 145.

22. Q. Li, B. Guo, J. Yu, J. Ran, B. Zhang, H. Yan and J. R. Gong, *J. Am. Chem. Soc.*, 2011, **133**, 10878.

List of Tables

Table 1. Morphological properties and band gap energies of CdS, Au/CdS, and CdS-A nanorods

Samples	Length (nm)	Thickness (nm)	Band gap (eV)
CdS	244.3±41.8	19.8±2.6	2.36
Au-CdS	173.6±45.5	16.1±2.3	2.31
CdS-A	147.3±15.3	10.1±4.1	2.39

List of Figures

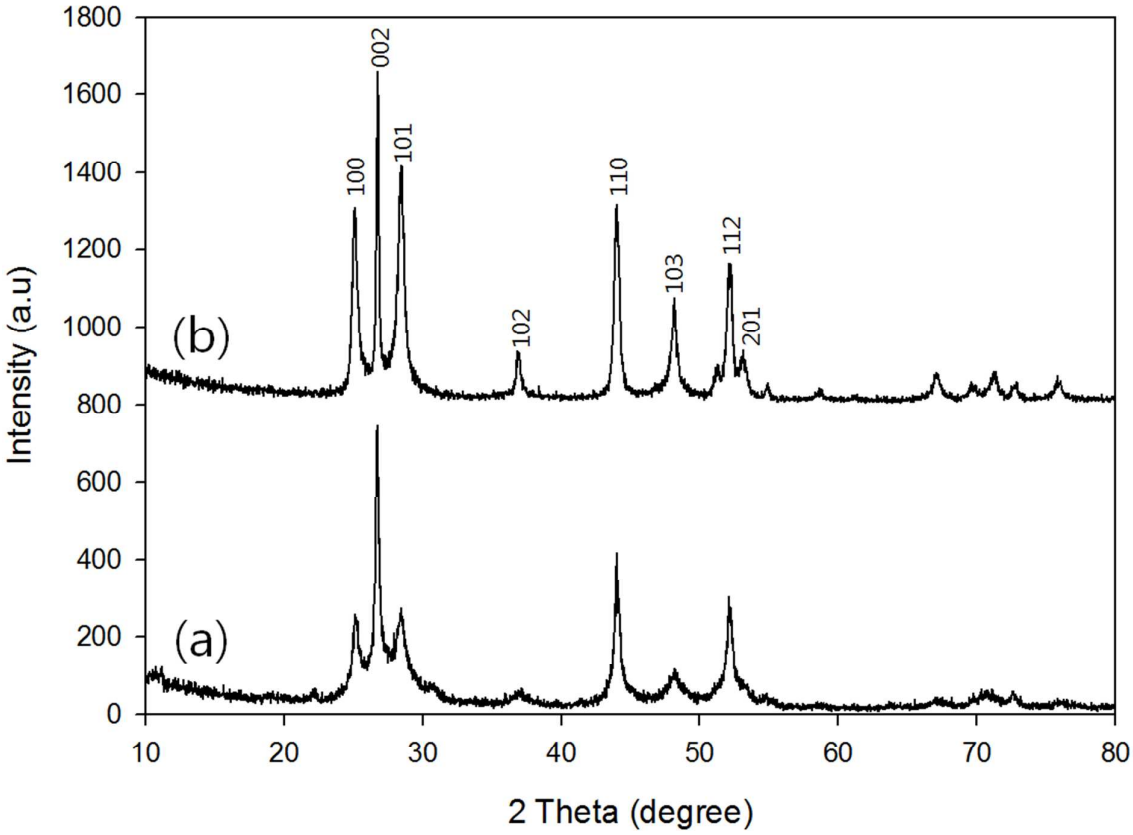

Fig. 1. XRD patterns of (a) CdS nanorods prepared by microwave-assisted method and (b) CdS-A nanorods prepared by conventional hydrothermal method using autoclave.

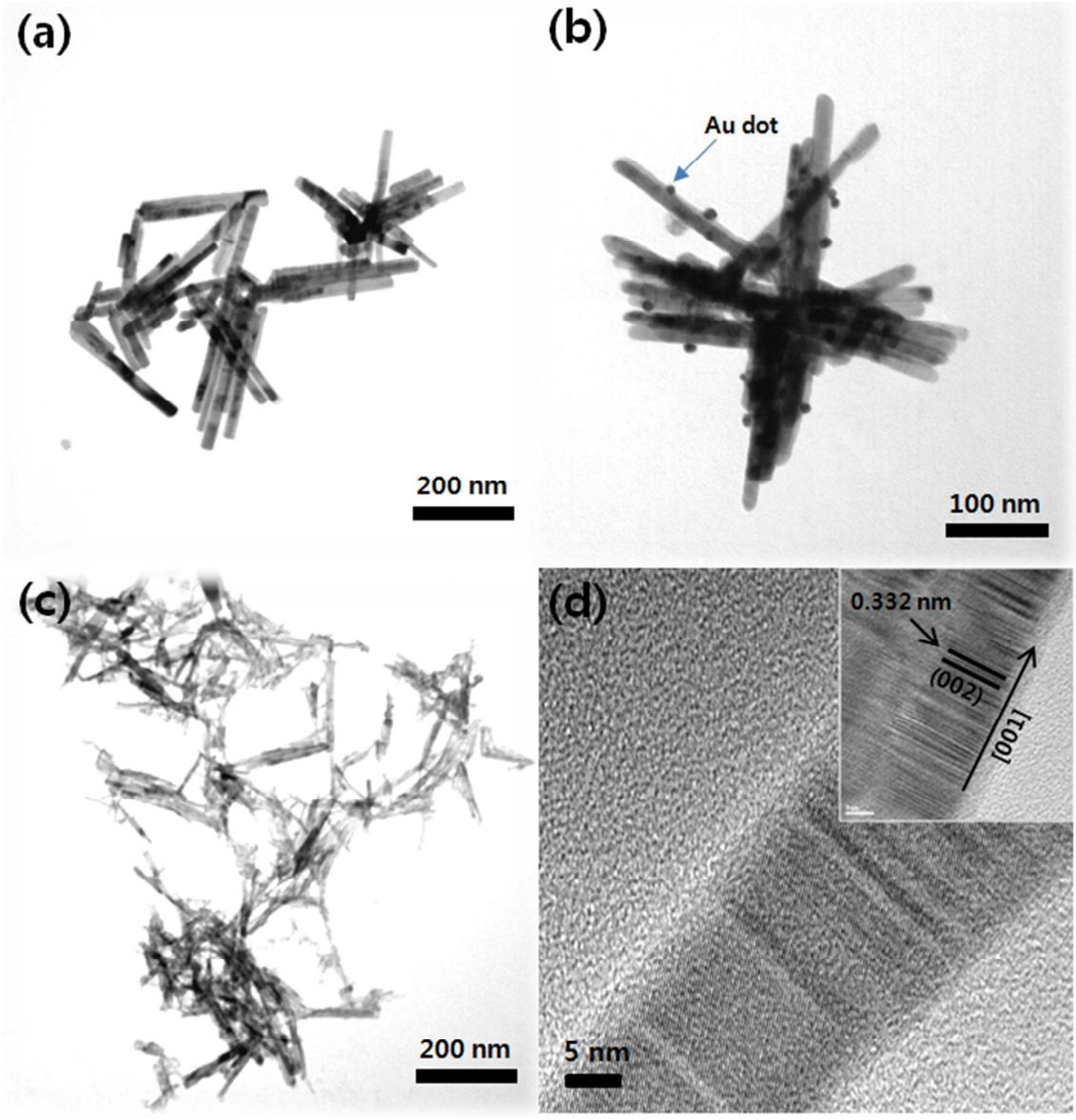

Fig. 2. TEM images of (a) CdS, (b) Au/CdS, and (c) CdS-A nanorods. (d) HR-TEM images of CdS nanorod.

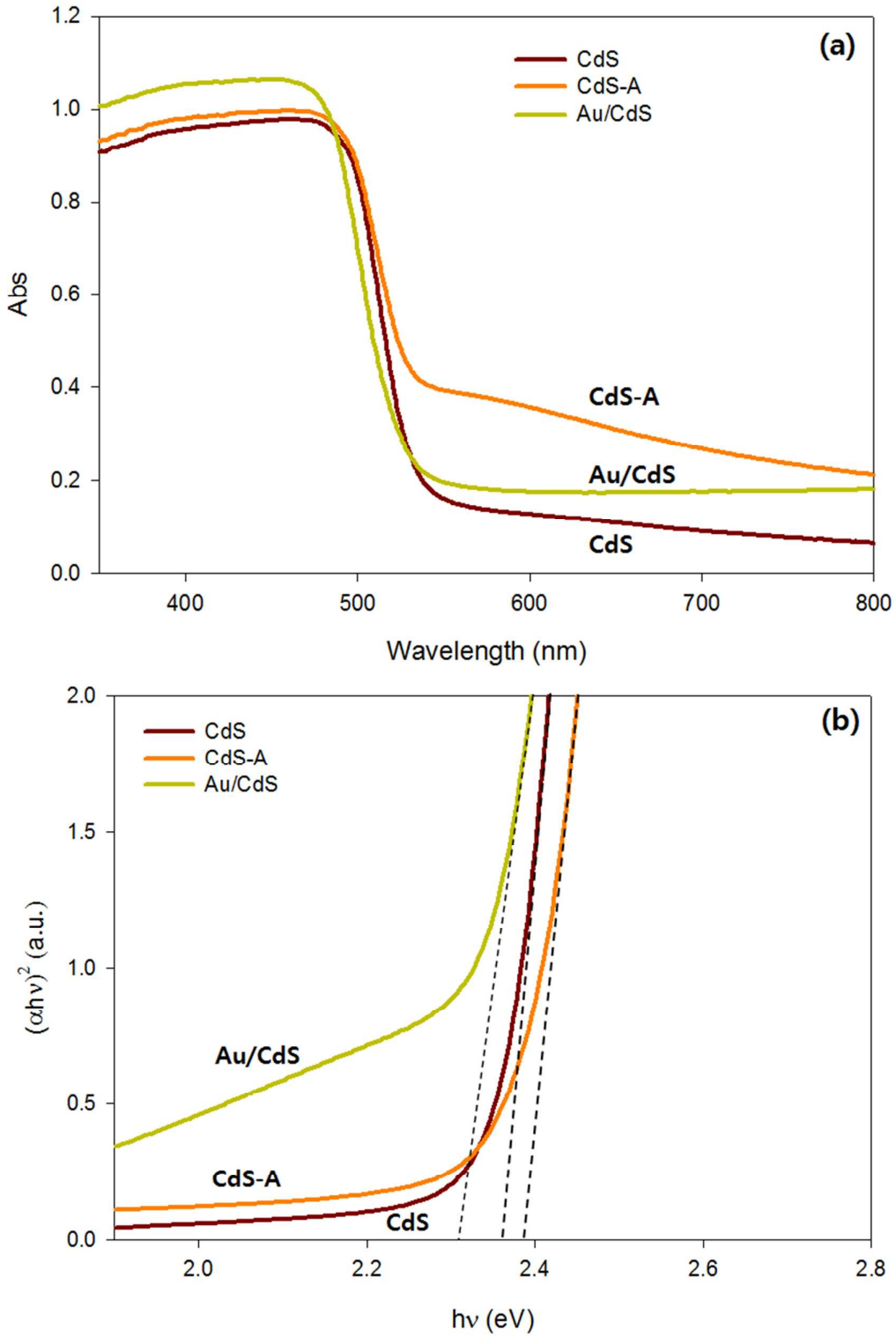

Fig. 3. (a) UV-DRS spectrum and (b) band gap energies estimated by $(\alpha h\nu)^2$ versus the photo energy ($h\nu$) of CdS, Au/CdS and CdS-A nanorods.

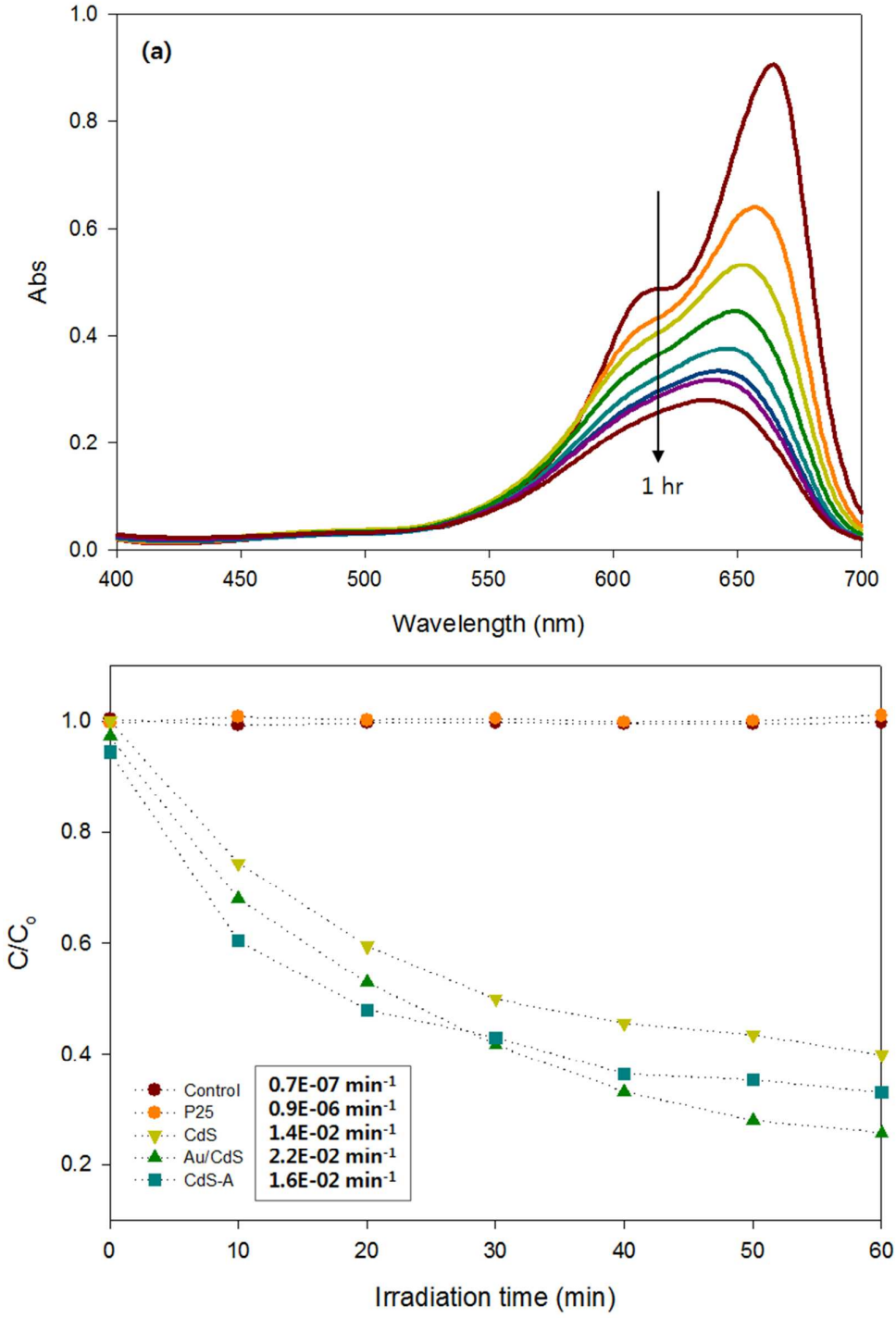

Fig. 4. (a) Time dependent UV-vis absorption spectrum of MB (C_o= 10 mg/L) in the presence of Au/CdS, and (b) variation of normalized (C/C_o) concentration of MB (C_o= 5 mg/L) with irradiation time under visible-light condition. Inset box in (b) is kinetic rate constant of the pseudo first-order reaction.

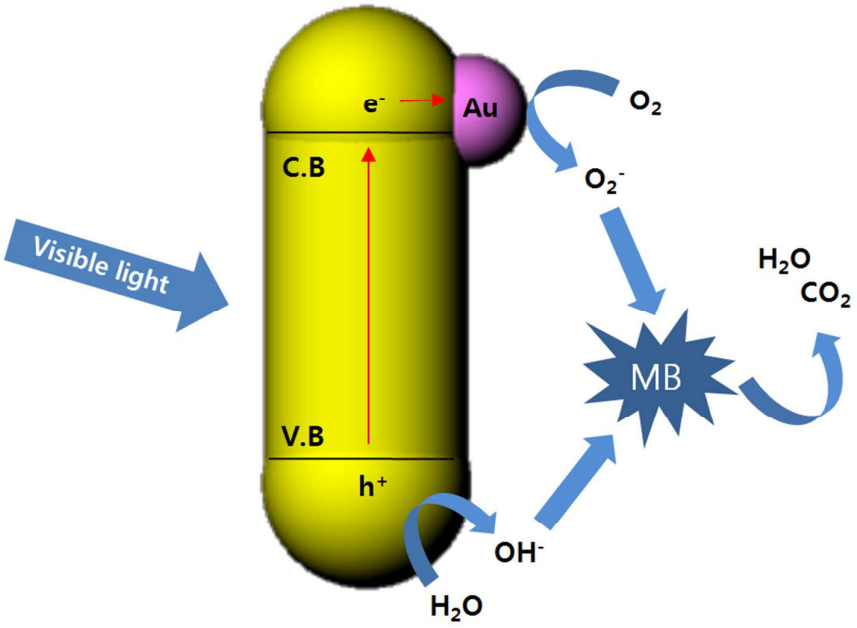

Fig. 5. Schematic illustration of photodegradation mechanism of MB by Au/CdS nanorods under visible-light irradiation.

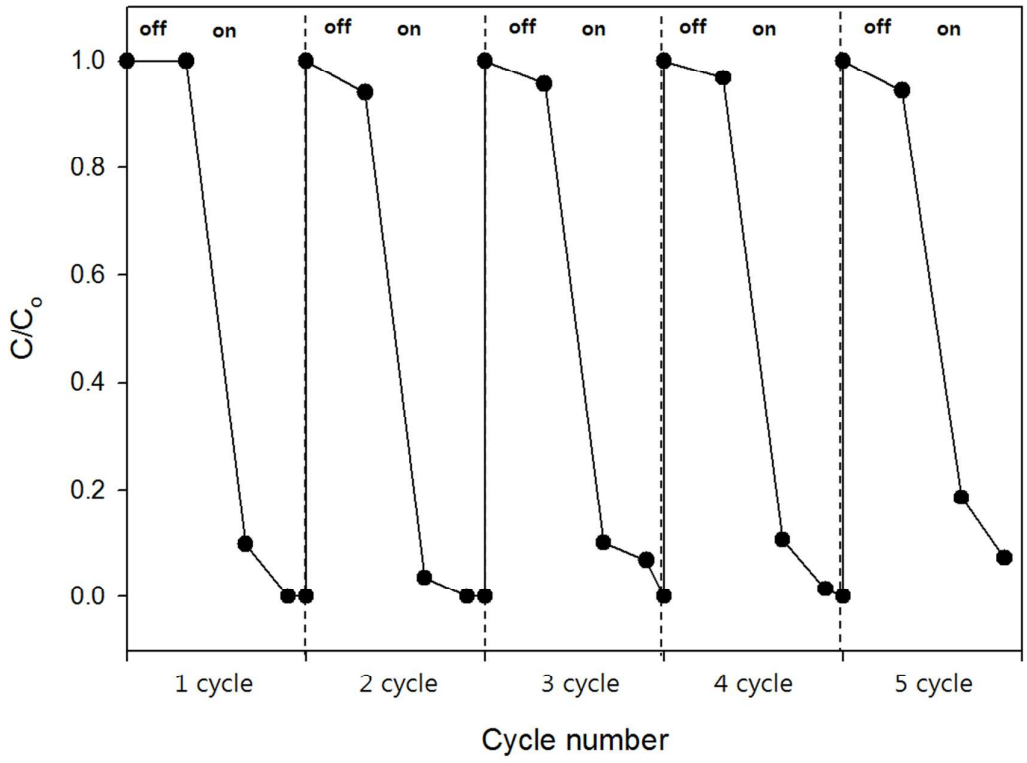

Fig. 6. Five-cycle photodegration test of Au/CdS nanorod for MB (3 mg/L).